Geosci. Model Dev. Discuss., 4, 1723–1754, 2011
www.geosci-model-dev-discuss.net/4/1723/2011/
doi:10.5194/gmdd-4-1723-2011
© Author(s) 2011. CC Attribution 3.0 License.

Geoscientific Model Development Discussions

This discussion paper is/has been under review for the journal Geoscientific Model Development (GMD). Please refer to the corresponding final paper in GMD if available.

Application of CMAQ at a hemispheric scale for atmospheric mercury simulations

P. Pongprueksa[1], C. J. Lin[2,3], P. Singhasuk[4], L. Pan[5], T. C. Ho[1], and H. W. Chu[5]

[1]Lamar University, Department of Chemical Engineering, Beaumont, Texas, USA
[2]Lamar University, Department of Civil Engineering, Beaumont, Texas, USA
[3]College of Environmental Science & Engineering, South China University of Technology, Guangzhou, China
[4]Lamar University, Department of Industrial Engineering, Beaumont, USA
[5]Lamar University, Department of Mechanical Engineering, Beaumont, USA

Received: 24 June 2011 – Accepted: 25 July 2011 – Published: 1 August 2011

Correspondence to: P. Pongprueksa (pruek.pongprueksa@lamar.edu)

Published by Copernicus Publications on behalf of the European Geosciences Union.

Abstract

Application of a regional model to study of fate and transport of a global pollutant such as mercury in the atmosphere can be challenging and improper usage of models may lead to questionable results. The difficulties in such application stem from the fact that regional models are usually used in relatively small domains and rely heavily on initial and boundary conditions (IC/BC) provided by global models where atmospheric physics and chemical mechanisms are generally diverse. This problem is particularly apparent for a persistent air pollutant such as mercury. In this study, a conventional application of the CMAQ (Community Multi-scale Air Quality) modeling system on regional scale was extended towards a hemispheric scale. Two simulations were performed using different IC/BC obtained from two global models. In terms of model evaluation, aircraft measurements of total gaseous mercury (TGM) concentration as well as mercury concentration and deposition data from ground-based measurements were used altogether in comparisons with the model simulations. The model results suggested an improvement in performance, as evidenced by a better circulation of the pollutant in Northern hemisphere relative to regional-scale simulations performed in our previous work. In this study, the simulation results using the two different inputs were found to be convergent as the simulation time progressed. The model results also suggested that BC has much weaker influence on the simulation results in a hemispheric domain than that on our previous regional assessment where BC was found to be one of the most important factors. In addition, mitigations of influences from IC/BC on model results in a hemispheric domain and implication of peaks of TGM concentration evident in aircraft measurement are also discussed.

1 Introduction

Mercury (Hg) exists in the environment in several forms, all of which can cause toxic effects or Hg poisoning depending upon its exposures and dosages. The environment

GMDD
4, 1723–1754, 2011

and human health concerns of Hg are primarily due to its organic compounds as well as ingestion of Hg-containing organisms and bioaccumulation in food chains. The atmosphere is an important reservoir through which Hg is distributed worldwide, mobilizing pollution to remote terrestrial and aquatic systems. Despite discoveries of state-of-the-science regarding mercury in the past decades, some significant links in our knowledge of atmospheric Hg cycles remain missing. The limitations are caused largely by the scarceness of existing observational data, lack of chemical speciation methods for ultra-trace Hg compounds in the atmosphere (at pptv and ppqv levels), and understanding in atmospheric chemistry of Hg. Recently, progress in measurement techniques has enabled extensive aircraft measurements of Hg distributing in the upper troposphere and lower stratosphere (Swartzendruber et al., 2009; Talbot et al., 2008; Radke et al., 2007; Banic et al., 2003; Friedli et al., 2004; Ebinghaus and Slemr, 2000; Slemr et al., 2009). These proceeding studies would lead to a better understanding of Hg cycling in the atmosphere.

Atmospheric Hg modeling studies have been conducted by using global or hemispheric scale models (Selin et al., 2007; Dastoor and Larocque, 2004; Seigneur et al., 2004, 2009; Travnikov and Ilyin, 2009; Jung et al., 2009; Jaeglé et al., 2009; Dastoor and Davignon, 2009) while regional Hg models would be used for more spatially resolved (finer resolution) results. The CMAQ (Community Multi-scale Air Quality) modeling system has been applied extensively to study chemical transport in the atmosphere ranging from regional scale to inter-continental scale (Wang et al., 2009; Bullock and Brehme, 2002; Lin et al., 2010; Pongprueksa et al., 2008; Lin and Tao, 2003; Gbor et al., 2007, 2006; Bullock et al., 2008; Lin et al., 2007; Sillman et al., 2007). Atmospheric Hg studies using CMAQ have been typically conducted in a series of steps. The first step is to simulate atmospheric Hg using either global or hemispheric scale model. The outputs from those models are then used as the inputs for CMAQ model simulation (downscaling method) in the later step. An advantage of CMAQ model over some global Hg models is the fully-coupled of chemistry treatment (or online treatment) where atmospheric constituents (e.g. gases, radicals, and particulates) used in

GMDD
4, 1723–1754, 2011

Hg chemical reactions are directly calculated from emission inventories instead of relying on concentrations generated by external models. This online treatment is essential due to the fact that most atmospheric oxidants plays an important role in determining fate of a trace gas, such as atmospheric Hg, even though it is not the case of vice versa. To date, the application of CMAQ on the chemical transport of Hg has been limited to regional scale.

A major limitation in regional Hg simulations is their dependency on initial and boundary conditions (IC/BC), typically generated from global models. Model simulations in regional scale such as a CONUS domain were greatly affected by BC as reported in a previous study by Pongprueksa et al. (2008). Bullock et al. (2008, 2009) also performed an inter-comparison of mercury models using several downscaling combinations of three regional models (i.e. CMAQ, REMSAD, and TEAM) and three global models (i.e. CTM, GEOS_Chem, and GRAHM) in a North America domain (NAMMIS). The study in 2009 demonstrated a very strong impact of the BC obtained from global models. The model performance comparisons for all three regional models paired with each of the inputs from three different global models showed the same trend confirming significant effect of BC from different global models on regional-scale simulation results. In this study, application of CMAQ on a hemispheric scale is demonstrated in effort to reduce uncertainties in regional-scale simulation caused by IC/BC derived from different modeling platforms. The slow air exchange between the Northern and Southern hemispheres estimated to be about 1 yr (World Meteorological Organization, 1985) would allow simulations in a hemispheric scale to be less affected by BC which may be originated from a foreign model. A subsequent BC derived from a model simulated in the hemispheric scale (Northern or Southern) would be more appropriate for simulations in regional/local domain sharing the same modeling platform. In contrast, influences of BC may not be greatly reduced with Western or Eastern hemispheric applications where a significantly faster air exchange (in terms of weeks) between the two hemispheres is evident. The influences of IC can be weakened by using a proper model "spin-up" period or launching the model simulation prior to the interested time

GMDD
4, 1723–1754, 2011

frame. Therefore, outputs from a hemispheric CMAQ simulation will provide direct downscaling for succeeding simulations in regional and local scales. This approach can eliminate discrepancies in model chemistry (chemical mechanism and homogeneous/heterogeneous phase treatments), model physics (transport and deposition), and model configuration (e.g. temporal distribution and vertical layer description).

The objectives of this study are to: (1) apply CMAQ-Hg) for simulations in a North Hemispheric domain, (2) evaluate the model performance using surface and aircraft measurements of Hg, and (3) explain the elevated Hg concentrations from the aircraft measurement using model results. The Hg measurement from ground-based and aircraft measurements in North America, Europe, and the East Asia during 2005 are used for the model performance evaluation, which provides insights to the model's capability. The ground-based measurements include CAMNet (the Canadian Atmospheric Mercury Measurement Network), EANET (the Acid Deposition Monitoring Network in East Asia), EMEP (the European Monitoring and Evaluation Programme), and MDN (the Mercury Deposition Network). Aircraft measurements of total gaseous mercury (TGM) from the CARIBIC project (Civil Aircraft for Regular Investigation of the atmosphere Based on an Instrumented Container) (Slemr et al., 2009) were also incorporated in this study.

2 Methodology

2.1 Model input data

The meteorological inputs needed for simulating the Weather Research and Forecasting modeling system (WRF) were obtained from the Global Forecast System (GFS) data that are generated by the NCEP (National Centers for Environmental Prediction) with 1-degree spatial and 6-hour temporal resolution (ds083.2) (National Center for Atmospheric Research, 2009). Clear sky photolysis rates of gases are calculated using satellite measurement of ozone column from the NASA Total Ozone Mapping Spectrometer (TOMS) (McPeters, 2009).

GMDD
4, 1723–1754, 2011

Two sets of IC and BC (Hg species only) derived from the outputs of two global mercury transport models were used. The two models are the Global/Regional Atmospheric Heavy Metals (GRAHM) model (Dastoor and Larocque, 2004; Ryzhkov, 2009; Dastoor and Davignon, 2009) and the Global EMEP Multi-media Modelling System (GLEMOS) (Travnikov et al., 2010) which is a global model version developed from the Meteorological Synthesizing Centre-East's Hemispheric model of Heavy Metal atmospheric transport (MSCE-HM-Hem) (Ryaboshapko et al., 2007; Travnikov, 2005; Travnikov and Ilyin, 2009). A vertical profile comparison of the IC/BC data from the two global models is shown in Fig. 1. Figure 1a shows the arithmetic mean of IC for the entire CMAQ domain while Fig. 1b shows the annual average of BC at different vertical layers of the model.

Mercury emissions are based on global anthropogenic Hg emissions (AMAP/UNEP, 2008) and the emissions by natural processes (Lin et al., 2005; Seigneur et al., 2004). The total Hg emission of 4172.1 Mg yr^{-1} in our hemispheric domain includes elemental Hg (3632.6 Mg yr^{-1}), divalent Hg (427.9 Mg yr^{-1}), and particulate-bound Hg (111.6 Mg yr^{-1}). Non-mercury emissions are obtained from pre-gridded emission data of aerosol/gas species (Heil and Schultz, 2009). A brief comparison of the Hg models used in this study and their Hg emission estimates are provided in Table 1. More detailed information is provided elsewhere (Travnikov et al., 2010).

2.2 Observation networks

Observational data used in the model performance evaluation were obtained from aircraft and ground measurements in the Northern Hemisphere. The static pressure and TGM concentration were extracted from the CARIBIC data. The observed static pressure was also used to determine the corresponding model altitude in model evaluation. The CARIBIC is a project to monitor and study chemical and physical processes in the Earth's atmosphere (upper troposphere and lower stratosphere). The measurements have been made during long distance flights of a commercial airline since 2004 using automated instrumentations in the freight container with a sampling inlet underneath

GMDD
4, 1723–1754, 2011

the airplane. The ground measurement networks include CAMNet, EANET, EMEP, and MDN. These networks measure precipitation, atmospheric Hg species concentrations, and Hg wet deposition in North America, Europe, and East Asia. A brief description of these networks is summarized in Table 2. The ground-based monitoring sites and simplified CARIBIC flight trajectories within the CMAQ modeling domain are shown in Fig. 2.

2.3 Model configuration

Meteorological data were generated using the Advanced Research WRF (ARW) version 3.1.1 (Wang et al., 2010). The key configurations for ARW include Kain-Fritsch scheme cumulus parameterization, WRF Single-Moment 6-class microphysics, Rapid Radiative Transfer Model (RRTM) long-wave radiation, Dudhia short-wave radiation scheme, Pleim-Xiu land surface model and surface layer, and ACM2 (Asymmetric Convective Model) planetary boundary layer. The ARW outputs were processed using MCIPv3.4.1 (Byun and Ching, 1999; Otte and Pleim, 2010) to generate model-ready meteorology for chemical transport simulations.

CMAQ v4.6 (Byun and Schere, 2006; Byun and Ching, 1999) was applied for assessment of atmospheric Hg in a Northern Hemispheric domain. The model is based on a three-dimensional Eulerian atmospheric chemistry and transport modeling system that simulates Hg, ozone, particulate matter, acid deposition, and visibility simultaneously. The model components and sciences have been documented elsewhere (Bullock and Brehme, 2002; Bullock et al., 2008; Travnikov et al., 2010). A spin-up period of 10 days is used to eliminate the impact of initial conditions for atmospheric oxidants (e.g. O_3, OH, and H_2O_2 etc.) that react with mercury. As for mercury species, global models were simulated for several years prior to the study period (2005) in order to provide the initial and boundary conditions of them in this study.

A hemispheric model domain with a Polar Stereographic projection at 108-km spatial resolution and 187×187 grid cells was used (Fig. 2) for this experiment. The CARIBIC flight trajectories in the model domain are between São Paulo (GRU) and

GMDD
4, 1723–1754, 2011

Frankfurt (FRA), between Frankfurt and Guangzhou (CAN), and between Guangzhou and Manila (MNL). The actual CARIBIC flight trajectories and the simplified tracks (with its equations) for model data extraction are shown in Fig. 3.

3 Results and discussion

3.1 Preliminary evaluation

Identifying the model characteristics of a regional model can be achieved by running the model using multiple sets of IC/BC. Therefore, CMAQ-Hg simulations were performed using two sets of IC/BC in two simulation cases. Case 1 refers to CMAQ results using the IC/BC from GRAHM, while Case 2 is the simulation of CMAQ that used the IC/BC from GLEMOS.

Figure 4 shows the comparisons of observational and model-predicted annual averages of precipitation and aqueous Hg concentration in 2005. Annual medians of the measured and model-simulated precipitation differed by <4 % (1.9–3.9 %) and the difference of annual means varied from 2.7 % to 15.7 %. The simulated precipitations agreed reasonably well with the measurements (Fig. 4a), while the difference between the observed and simulated aqueous Hg concentrations is more substantial (Fig. 4b). Generally, Case 1 was somewhat underestimated in terms of the measured concentrations for both MDN and EMEP sites and Case 2 produced greater concentrations than Case 1. Case 1 gave slightly better aqueous Hg concentration at EMEP sites compared to Case 2 in terms of data distribution. However, the percent error of mean of aqueous Hg concentration ranged from 3.2 % to 12.0 % in Case 2, while Case 1 had much larger percent error values (7.4–32.0 %). Comparing with an earlier model study by Lin et al. (2007), the model simulation in the hemispheric scale (especially Case 2) yielded a more favorable result than that from the application of CMAQ on a regional scale.

GMDD
4, 1723–1754, 2011

Figure 5 shows plots of Hg concentrations from the model results versus those from ground-based (annual average) and aircraft (daily average) measurements together in 2005. In all regions, Case 2 provided a better estimate for Hg concentrations than that from Case 1, except for the group of Hg^P and Hg^{II} concentrations at the EMEP sites (we grouped them together due to the limited of monitoring sites available). To compare the CMAQ-Hg results with CARIBIC data, the 15-min CARABIC data are processed into hourly average. Recorded static pressure during the flights is used to match the model altitude in order to compare the observed TGM concentrations with the simulated ones. Both simulation cases yielded results of TGM concentration that are comparable and in agreement with the CARIBIC measurements with the results of Case 2 (error of median and mean are 3.1 % and 4.2 %) being slightly better than that of Case 1 (error of median and mean are 5.4 % and 4.9 %). TGM and Hg^0 concentrations estimated by Case 2 agreed more closely to the CAMNet and EMEP measurements (error of median and mean range 0.1–0.2 % and 2.6–5.0 %) compared with Case 1 (error of median and mean range 6.3–6.6 % and 9.1–11.5 %). The simulated Hg^P and Hg^{II} concentrations at EMEP sites show that results from Case 1 reproduced the ground measurements more favorable than those from Case 2. Differences in concentration from the two simulation cases are caused by the different IC/BC implemented. The IC/BC re-gridded from GLEMOS model output has higher background concentrations of Hg^P compared with the values from the GRAHM model. Similarly, higher background concentrations of TGM, Hg^0, and Hg^T estimated by Case 1 are caused by higher concentrations at locations near monitoring sites generated by the GRAHM model.

The two simulation cases produced similar outputs in terms of TGM, Hg^0, and Hg^T concentrations. In this study, the Relative Percentage Difference (RPD, %) was used as a comparison index for the two sets of model results which are equally important. The RPD of two simulation values, x and y, can be calculated by dividing the absolute difference of the two values by the sum of the same two values and multiplying with 200. The equation of RPD is

GMDD
4, 1723–1754, 2011

$$\mathrm{RPD},\% = 200 \times \left| \frac{x-y}{x+y} \right|. \quad (1)$$

The Relative Percentage Difference (RPD) of mean and median for concentrations between the two cases are smaller than 10 % except for the group of Hg^P and Hg^{II}, and total Hg in precipitation. The higher RPDs of Hg^P and Hg^{II} (36.1 % and 38.4 % for mean and median at EMEP sites) and total Hg in precipitation (10.8–25.7 % and 28.3–33.6 % for mean and median at EMEP and MDN sites) suggest that Hg^P or Hg^{II}, and total Hg in precipitation are more sensitive to IC/BC. The concentrations of Hg^0, the dominant species (TGM and Hg^T), are relatively constant when compared with that of the other Hg species (Hg^P and Hg^{II}). Therefore, concentrations of Hg^P, Hg^{II}, and total Hg in precipitation should be better criteria in Hg model evaluation than TGM, Hg^0, and Hg^T. One should note that higher TGM, Hg^0, and Hg^T concentrations in IC/BC do not always result in higher Hg concentration in precipitation because Hg^0 has a very small solubility when compared with Hg^{II}. Higher Hg^{II} or Hg^P concentration would directly link to higher Hg concentration in precipitation. However, the number of atmospheric Hg monitoring sites is still limited (particularly for speciated Hg measurements) and additional continuous observations of mercury concentrations especially in Asia (a major source region) are required for a more comprehensive model evaluation.

3.2 The entire domain comparison between two simulation cases

Differences in annual average TGM concentration between the two simulation cases are small in most part of the Northern Hemispheric domain as depicted in Fig. 6. Figure 6a and b show annual average of TGM concentrations at ground-level from GRAHM-CMAQ (Case 1) and GLEMOS-CMAQ (Case 2), respectively. Spatial patterns of TGM from both simulation cases are comparable but the TGM concentrations from GRAHM-CMAQ are slightly higher than that from GLEMOS-CMAQ. TGM concentrations at ground-level are elevated in regions with major anthropogenic sources while TGM concentrates near the North Pole and decreases with the latitude at the average

GMDD
4, 1723–1754, 2011

aircraft measurement level (or flight-level, altitude ~10 km a.m.s.l.). Figure 6c and d show annual average of TGM concentrations at the CARIBIC flight-level from GRAHM-CMAQ and GLEMOS-CMAQ, respectively. At the average flight-level, concentrations from the two simulations are similar and the spatial distributions are relatively uniform without elevated TGM concentration being evident. The overall TGM concentrations from GLEMOS-CMAQ are smaller than the results from GRAHM-CMAQ. The differences in TGM concentration from the two cases are greater at the flight-level (ca. 0.1–0.4 ng m^{-3}) compared with those at surface level (ca. 0.1 ng m^{-3}). The discrepancies are mainly caused by the use of different sets of IC/BCs as discussed earlier. In addition, GRAHM produces higher TGM or Hg^0 levels compared with the results from GLEMOS because of differences in chemical mechanism between the two global models mainly due to the facts that: (1) GRAHM does not include the oxidation of Hg with OH in gas phase while GLEMOS does, and (2) GRAHM incorporates the photoreduction of Hg in aqueous phase while GLEMOS does not (Travnikov et al., 2010). Therefore, GLEMOS requires slightly more Hg emission estimates to balance Hg budget in the atmosphere. In summary, the chemical mechanism in GRAHM is less oxidizing, leading to greater TGM concentrations.

3.3 CARIBIC aircraft data and CMAQ model results

3.3.1 Distribution of TGM concentration

Figure 7 compares CMAQ simulation results to the CARIBIC data (TGM and static pressure) in the upper troposphere corresponding to longitude along the CARIBIC flight path (x-axis) and day of year (y-axis) within the Northern Hemisphere domain (Fig. 2). The plot visualizes both spatial and temporal changes during the modeling period in order to show seasonal variation of TGM concentration.

Figure7a is constructed by assuming the measured TGM as a representative of the daily average. The TGM data (May 2005 to March 2007) are plotted in bubbles and missing data are calculated using the Delaunay triangular interpolation for every 1° of

GMDD
4, 1723–1754, 2011

longitude and between flight intervals. Peaks of daily average TGM concentrations appear around the transition of spring/summer and in fall near the flight destination in Europe (FRA). For the locations near flight destinations in Asia (CAN and MNL), the peaks of daily average TGM concentration are detected in May and September. At locations far away from the flight destinations, the average TGM concentrations are low ($<1\,ng\,m^{-3}$) especially in summer.

Figure 7b shows the static pressure during the CARIBIC flights. High static pressures were measured near the flight destinations during takeoffs and landings. The static pressure partially explains TGM concentration variation as the concentrations tend to decrease with increasing altitude. Typically, Hg^0 decreases as altitude increases (or pressure decreases) while Hg^{II} typically increases with altitude (Swartzendruber et al., 2009). Several measurement studies (Radke et al., 2007; Talbot et al., 2008; Swartzendruber et al., 2009; Friedli et al., 2004) have also reported a similar relationship of the altitude/pressure and TGM/Hg^0 concentrations.

To compare CMAQ results with those from CARIBIC data, daily average TGM concentrations from the CMAQ using IC/BC from the GRAHM or the GLEMOS are extracted from the flight path and plotted at every 1° of longitude for the entire year. Figure 7c and d shows the model results along the flight paths. Both cases show similar TGM concentrations, with Case 1 having slightly higher values. The maximum values (peaks) of daily average TGM concentration of the year at each longitude are highlighted in bubbles. Higher TGM concentrations occurred in November and December over Europe, while the same situation occurred in summer (June–August) and the starting of fall (September) over Asia. Generally, both model cases could not capture the high TGM concentrations observed during CARIBIC flights in Europe but the model results did capture some Asian plumes. A close look into the meteorological data shows that a combination of stagnant air (wind speed $<0.5\,m\,s^{-1}$) and lack of precipitation is associated with the elevated concentrations, indicating mercury emitted from anthropogenic and natural sources accumulates in the air column due to the lack of horizontal dispersion.

GMDD
4, 1723–1754, 2011

With a small temporal variation of Hg emissions, the daily average TGM concentrations from simulations should remain relatively uniform for the same longitude on daily basis. Therefore, the same color representing TGM concentration would appear in perpendicular to the x-axis (longitude). However, both observation and simulation results show remarkable peaks over Asia (see Fig. 7) instead of a homogeneous color strip pattern.

3.3.2 An evidence of air stagnation

To further examine the annual peaks of daily average TGM concentration along the CARIBIC flight trajectories, vertical concentration profiles at the locations corresponding to peaks (bubbles in Fig. 7c and d) are extracted from model outputs as shown in Fig. 8. The extracted vertical profiles are plotted with model vertical grid levels (sigma-level or altitude above mean sea level) in y-axis while the x-axis indicates the longitude of the flight trajectories. Both cases show a similar vertical pattern with a trend of TGM concentrations decreasing with increasing altitude in these regions and the elevated TGM concentrations at the upper layers are originated from the near surface emissions. This is possibly due to the greater vertical dispersion when the horizontal movement is limited. The correlation in pattern suggests that daily TGM peaks shown in Fig. 7 are caused by air stagnation.

3.3.3 Implications of IC/BC

The impacts of IC/BC on a model-simulated concentration of mercury are different depending upon its species (Hg^0, Hg^{II}, or Hg^P). Pongprueksa et al. (2008) demonstrated that BC was more important relative to IC in a regional-scale simulation since the initial air mass could be replaced by the inflow within a short period of time. In contrast, IC (especially for inert species such as Hg^0) would become more important for a hemispheric-scale simulation because most of the circulation would occur within the domain. To further address the impact of IC/BC, the simulation results are compared using the Relative Percentage Difference (RPD, %).

GMDD
4, 1723–1754, 2011

Figure 9 shows RPD between Case 1 and Case 2 results along the aircraft trajectories (x-axis) for the entire year. The RPD values for TGM and Hg^0 have a similar pattern (Fig. 9a and b) because Hg^0 is the dominant species of atmospheric mercury. Greater RPD values are evident during model starting periods and locations close to the model boundaries (longitude <0° and longitude >90°). The RPD values of Hg^{II} are greater than the values of Hg^0 but much smaller than those of Hg^P (Fig. 9c and d). Moreover, RPD values for Hg^{II} and Hg^P can also be affected by TGM or Hg^0 concentrations. In CMAQ, Hg^P is assigned to fine particulate mode and therefore has a greater atmospheric lifetime compared to that of Hg^{II}. The Hg^P produced from the oxidation of Hg^0 lead to the similar pattern found in Fig. 9b and d. The high RPD values in the early simulation period (the first 4 months) are caused by differences in the initial conditions while the high values near model domain boundaries are caused by the boundary conditions derived from the two completely different models. Due to the short atmospheric lifetime of Hg^{II}, the effect of IC sustains only for a few days (Fig. 9c) and boundary effect is not obvious, consistent with the previous study results by Pongprueksa et al. (2008).

The RPD values gradually decrease over time. The means of RPD for TGM and Hg^0 across the flight path in the domain reduce from 32.2 % at the start to 6.8 % toward the end of the year. Consequently, a model spin-up period of one-year (or longer) is recommended to reduce the influences from initial conditions of Hg^0. Model spin-up periods required for Hg^{II} and Hg^P (ranging from days to a few months) are much shorter than that for Hg^0, hence the spin-up for Hg^0 is the governing period for simulations on hemispheric scale. The influence of BC can be indentified at locations where the RPD values are high (near domain boundaries). The high values persist even after several months of simulation. It is therefore important that the model region of interest be sufficiently remote from domain boundaries. In our hemispheric simulations, the impacts of BC are small at the locations above 20° N of latitude.

GMDD
4, 1723–1754, 2011

3.4 Future model improvement

Results of model simulations can be improved by using either model input data which is better representing environmental conditions or a better model configuration which can also be as challenging as adding new multi-media chemical schemes. The meteorological fields and model input data can be improved using several methods such as using nudging-based data assimilation to reproduce the actual characterization of the atmosphere. Improved meteorological fields provide assurance in succeeding emissions processing and air quality simulations. Due to large area coverage, emission estimations in the North Hemisphere may be highly uncertain therefore the updated emission inventories are always favorable toward better estimations.

Mercury species concentrations varied significantly depending on the altitude and atmospheric pressure based on CARIBIC data. Therefore, model simulations using a finer vertical resolution (especially at flight-level) would compared more favorably with aircraft measurements in the free troposphere and lower stratosphere. In addition, incorporating important chemical reactions such as reactions with reactive bromine species (Holmes et al., 2006, 2010) would also be beneficial.

We found that application of CMAQ-Hg in the hemispheric domain shows model improvements over earlier CMAQ-Hg modeling efforts at regional scale. In a regional domain, model results are continuously influenced by BC. Because the global models used for generating the BC typically have different science configuration compared to a regional model such as CMAQ-Hg, there is a potential that the model results can be biased by the input data of IC/BC. By applying the model in a hemispheric domain, we demonstrate that the influences of initial condition can be excluded by model spin-up for a concerned pollutant with a relatively long atmospheric lifetime (Hg^0). The hemispheric model results of CMAQ-Hg can be directly applied in model nesting of regional and local model analysis, eliminating issues of model science inconsistency when performing model downscaling from a foreign global model. The impact of BC can reach up to 20° N, typically no farther than 10° N, in our experiments in the hemispheric

GMDD
4, 1723–1754, 2011

domain. This is appropriate for assessing mercury transport and deposition in most populated region in the North Hemisphere.

4 Conclusions

In this study, an extended application of CMAQ-Hg over the Northern Hemisphere in 2005 was performed. Model evaluation using both aircraft and ground measurements indicate that the hemispheric simulations can reasonably reproduce the concentration and deposition of atmospheric mercury. The two sets of IC/BC inputs derived from GRAHM and GLEMOS global models yielded comparable results relative to flight measurement (inputs from GRAHM and GLEMOS yielded 3.1 % and 5.4 % error in medians, and 5.7 % and 4.9 % error in means, respectively), with the case of inputs from GLEMOS being slightly better. The Relative Percentage Difference (RPD) of means and medians of TGM, Hg^0 and Hg^T concentrations are less than 10 %. This suggests resemblance in performance of the two simulations. The agreement in TGM concentrations at ground-level (0.1 ng m^{-3}) is stronger compared to those measured at flight-level (0.1–0.4 ng m^{-3}). The model results in both cases suggested that the downscaling effect of BC is greatly reduced on the hemispheric scale. Model simulations in such large scale benefit not only long atmospheric lifetime such as mercury but also short lifetime chemicals (e.g. O_3, NO_x, and SO_2 etc.). In addition, the elevated concentrations of TGM in East Asia are apparently caused by air stagnation.

Acknowledgements. We thank Oleg Travnikov for providing GLEMOS data, Ashu P. Dastoor and Andrew Ryzhkov for GRAHM data, Franz Slemr and Carl A. M. Brenninkmeijer for CARIBIC support, and Anne-Gunn Hjellbrekke for EMEP data. The authors acknowledge the National Atmospheric Deposition Program (NADP) for MDN data and the Canadian National Atmospheric Chemistry (NAtChem) database and its data contributing agencies/organizations for the provision of the CAMNet data used in the model evaluation. This work is supported in part by Texas Air Research Center. The funding support is gratefully acknowledged.

GMDD
4, 1723–1754, 2011

References

AMAP/UNEP: Technical background report to the global atmospheric mercury assessment, Arctic Monitoring and Assessment Programme/UNEP Chemicals Branch, 159, 2008.

Publications/EANET Acid Deposition Monitoring Network in East Asia: http://www.eanet.cc/product/index.html, access: 28 October 2010, 2010.

Banic, C. M., Beauchamp, S. T., Tordon, R. J., Schroeder, W. H., Steffen, A., Anlauf, K. A., and Wong, H. K. T.: Vertical distribution of gaseous elemental mercury in Canada, J. Geophys. Res.-Atmos., 108(D9), 4264, doi:10.1029/2002JD002116, 2003.

CARIBIC Lufthansa climate observation: http://www.caribic-atmospheric.com/index.htm, access: 7 May 2009, 2009.

Bullock, O. R. and Brehme, K. A.: Atmospheric mercury simulation using the CMAQ model: formulation description and analysis of wet deposition results, Atmos. Environ., 36, 2135–2146, 2002.

Bullock, O. R., Atkinson, D., Braverman, T., Civerolo, K., Dastoor, A., Davignon, D., Ku, J. Y., Lohman, K., Myers, T. C., Park, R. J., Seigneur, C., Selin, N. E., Sistla, G., and Vijayaraghavan, K.: The North American Mercury Model Intercomparison Study (NAMMIS): Study description and model-to-model comparisons, J. Geophys. Res.-Atmos., 113, D17310, doi:10.1029/2008JD009803, 2008.

Bullock, O. R., Atkinson, D., Braverman, T., Civerolo, K., Dastoor, A., Davignon, D., Ku, J. Y., Lohman, K., Myers, T. C., Park, R. J., Seigneur, C., Selin, N. E., Sistla, G., and Vijayaraghavan, K.: An analysis of simulated wet deposition of mercury from the North American Mercury Model Intercomparison Study, J. Geophys. Res.-Atmos., 114, D08301, doi:10.1029/2008JD011224, 2009.

Byun, D. and Schere, K. L.: Review of the governing equations, computational algorithms, and other components of the models-3 Community Multiscale Air Quality (CMAQ) modeling system, Appl. Mech. Rev., 59, 51–77, 2006.

Dastoor, A. P. and Larocque, Y.: Global circulation of atmospheric mercury: a modelling study, Atmos. Environ., 38, 147–161, 2004.

Dastoor, A. P. and Davignon, D.: Global mercury modelling at Environment Canada, in: Mercury Fate and Transport in the Global Atmosphere, edited by: Pirrone, N. and Mason, R., Springer US, 519–532, 2009.

Ebinghaus, R. and Slemr, F.: Aircraft measurements of atmospheric mercury over southern

GMDD
4, 1723–1754, 2011

and eastern Germany, Atmos. Environ., 34, 895–903, 2000.
The NAtChem/Toxics Request: http://www.msc.ec.gc.ca/natchem/toxics/request_e.html, access: 7 July 2009, 2005.
Friedli, H. R., Radke, L. F., Prescott, R., Li, P., Woo, J. H., and Carmichael, G. R.: Mercury in the atmosphere around Japan, Korea, and China as observed during the 2001 ACE-Asia field campaign: Measurements, distributions, sources, and implications, J. Geophys. Res.-Atmos., 109, D19S25, doi:10.1029/2003JD004244, 2004.
Gbor, P. K., Wen, D. Y., Meng, F., Yang, F. Q., Zhang, B. N., and Sloan, J. J.: Improved model for mercury emission, transport and deposition, Atmos. Environ., 40, 973–983, 2006.
Gbor, P. K., Wen, D. Y., Meng, F., Yang, F. Q., and Sloan, J. J.: Modeling of mercury emission, transport and deposition in North America, Atmos. Environ., 41, 1135–1149, 2007.
Juelich: ftp://ftp-ipcc.fz-juelich.de/pub/emissions/gridded_netcdf/, access: 13 October 2009, 2009.
EMEP Measurement data online: http://tarantula.nilu.no/projects/ccc/emepdata.html, access: 29 October 2010, 2010.
Holmes, C. D., Jacob, D. J., and Yang, X.: Global lifetime of elemental mercury against oxidation by atomic bromine in the free troposphere, Geophys. Res. Lett., 33, L20808, doi:10.1029/2006GL027176, 2006.
Holmes, C. D., Jacob, D. J., Corbitt, E. S., Mao, J., Yang, X., Talbot, R., and Slemr, F.: Global atmospheric model for mercury including oxidation by bromine atoms, Atmos. Chem. Phys., 10, 12037–12057, doi:10.5194/acp-10-12037-2010, 2010.
Jaeglé, L., Strode, S. A., Selin, N. E., and Jacob, D. J.: The Geos-Chem model, in: Mercury Fate and Transport in the Global Atmosphere, edited by: Pirrone, N. and Mason, R., Springer US, 533–545, 2009.
Jung, G., Hedgecock, I. M., and Pirrone, N.: The ECHMERT model, in: Mercury Fate and Transport in the Global Atmosphere, edited by: Pirrone, N., and Mason, R., Springer US, 547–569, 2009.
Lin, C.-J., Pongprueksa, P., Russell Bullock Jr, O., Lindberg, S. E., Pehkonen, S. O., Jang, C., Braverman, T., and Ho, T. C.: Scientific uncertainties in atmospheric mercury models II: Sensitivity analysis in the CONUS domain, Atmos. Environ., 41, 6544–6560, 2007.
Lin, C. J., Lindberg, S. E., Ho, T. C., and Jang, C.: Development of a processor in BEIS3 for estimating vegetative mercury emission in the continental United States, Atmos. Environ., 39, 7529–7540, 2005.

GMDD
4, 1723–1754, 2011

Lin, C.-J., Pan, L., Streets, D. G., Shetty, S. K., Jang, C., Feng, X., Chu, H.-W., and Ho, T. C.: Estimating mercury emission outflow from East Asia using CMAQ-Hg, Atmos. Chem. Phys., 10, 1853–1864, doi:10.5194/acp-10-1853-2010, 2010.

Lin, X. and Tao, Y.: A numerical modelling study on regional mercury budget for eastern North America, Atmos. Chem. Phys., 3, 535–548, doi:10.5194/acp-3-535-2003, 2003.

Ozone Data: http://toms.gsfc.nasa.gov/ozone/ozone_v8.html, access: 17 November 2009, 2009.

Sites in the NADP/MDN Network: http://nadp.sws.uiuc.edu/nadpdata/mdnalldata.asp, access: 29 October 2010, 2010.

Research Data Archive: http://dss.ucar.edu/datasets/ds083.2/, access: 11 November 2009, 2009.

Otte, T. L. and Pleim, J. E.: The Meteorology-Chemistry Interface Processor (MCIP) for the CMAQ modeling system: updates through MCIPv3.4.1, Geosci. Model Dev., 3, 243–256, 2010.

Pongprueksa, P., Lin, C. J., Lindberg, S. E., Jang, C., Braverman, T., Bullock, O. R., Ho, T. C., and Chu, H. W.: Scientific uncertainties in atmospheric mercury models III: Boundary and initial conditions, model grid resolution, and Hg(II) reduction mechanism, Atmos. Environ., 42, 1828–1845, 2008.

Radke, L. F., Friedli, H. R., and Heikes, B. G.: Atmospheric mercury over the NE Pacific during spring 2002: Gradients, residence time, upper troposphere lower stratosphere loss, and long-range transport, J. Geophys. Res.-Atmos., 112, D19305, doi:10.1029/2005JD005828, 2007.

Ryaboshapko, A., Bullock, O. R., Christensen, J., Cohen, M., Dastoor, A., Ilyin, I., Petersen, G., Syrakov, D., Travnikov, O., Artz, R. S., Davignon, D., Draxler, R. R., Munthe, J., and Pacyna, J.: Intercomparison study of atmospheric mercury models: 2. Modelling results vs. long-term observations and comparison of country deposition budgets, Sci. Total Environ., 377, 319–333, 2007.

Modeling of Atmospheric Mercury: http://redandr.ca/hg/2005/, access: 14 December 2009, 2009.

Seigneur, C., Vijayaraghavan, K., Lohman, K., Karamchandani, P., and Scott, C.: Global source attribution for mercury deposition in the United States, Environ. Sci. Technol., 38, 555-569, 2004.

Seigneur, C., Vijayaraghavan, K., Lohman, K., and Levin, L.: The AER/EPRI global chemi-

GMDD

4, 1723–1754, 2011

cal transport model for mercury (CTM-HG), in: Mercury Fate and Transport in the Global Atmosphere, edited by: Pirrone, N., and Mason, R., Springer US, 589–602, 2009.
Selin, N. E., Jacob, D. J., Park, R. J., Yantosca, R. M., Strode, S., Jaegle, L., and Jaffe, D.: Chemical cycling and deposition of atmospheric mercury: Global constraints from observations, J. Geophys. Res.-Atmos., 112, D02308, doi:10.1029/2006JD007450, 2007.
Sillman, S., Marsik, F. J., Al-Wali, K. I., Keeler, G. J., and Landis, M. S.: Reactive mercury in the troposphere: Model formation and results for Florida, the northeastern United States, and the Atlantic Ocean, J. Geophys. Res.-Atmos., 112, D23305, doi:10.1029/2006JD008227, 2007.
Slemr, F., Ebinghaus, R., Brenninkmeijer, C. A. M., Hermann, M., Kock, H. H., Martinsson, B. G., Schuck, T., Sprung, D., van Velthoven, P., Zahn, A., and Ziereis, H.: Gaseous mercury distribution in the upper troposphere and lower stratosphere observed onboard the CARIBIC passenger aircraft, Atmos. Chem. Phys., 9, 1957–1969, doi:10.5194/acp-9-1957-2009, 2009.
Swartzendruber, P. C., Jaffe, D. A., and Finley, B.: Development and First Results of an Aircraft-Based, High Time Resolution Technique for Gaseous Elemental and Reactive (Oxidized) Gaseous Mercury, Environ. Sci. Technol., 43, 7484–7489, 2009.
Talbot, R., Mao, H., Scheuer, E., Dibb, J., Avery, M., Browell, E., Sachse, G., Vay, S., Blake, D., Huey, G., and Fuelberg, H.: Factors influencing the large-scale distribution of Hg° in the Mexico City area and over the North Pacific, Atmos. Chem. Phys., 8, 2103–2114, doi:10.5194/acp-8-2103-2008, 2008.
Travnikov, O.: Contribution of the intercontinental atmospheric transport to mercury pollution in the Northern Hemisphere, Atmos. Environ., 39, 7541–7548, 2005.
Travnikov, O. and Ilyin, I.: The EMEP/MSC-E mercury modeling system, in: Mercury Fate and Transport in the Global Atmosphere, edited by: Pirrone, N., and Mason, R., Springer US, 571–587, 2009.
Travnikov, O., Lin, C.-J., Dastoor, A., Bullock, O. R., Hedgecock, I. M., Holmes, C., Ilyin, I., Jaeglé, L., Jung, G., Pan, L., Pongprueksa, P., Seigneur, C., and Skov, H.: Global and Regional Modeling, in: HTAP 2010 Assessment Report, edited by: Pironne, N. and Keating, T., 2010.
Wang, K., Zhang, Y., Jang, C., Phillips, S., and Wang, B.: Modeling intercontinental air pollution transport over the trans-Pacific region in 2001 using the Community Multiscale Air Quality modeling system, J. Geophys. Res., 114, D04307, doi:10.1029/2008JD010807, 2009.

GMDD
4, 1723–1754, 2011

Wang, W., Bruyère, C., Duda, M., Dudhia, J., Gill, D., Lin, H.-C., Michalakes, J., Rizvi, S., and Zhang, X.: Weather Research & Forcasting ARW: Version 3 Modeling System User's Guide, Apr. 2010 ed., National Center for Atmospheric Research, 350 pp., 2010.

World Meteorological Organization: Atmospheric ozone : an assessment of our understanding of the processes controlling its present distribution and change, Global Ozone Research and Monitoring Project. Report; No. 16, World Meteorological Organization, Geneva, 3 v. pp., 1985.

GMDD

4, 1723–1754, 2011

Table 1. Brief summary of model configurations and emission estimates.

Model	Scale	Horizontal grid resolution	Hg gas phase	Hg aqueous phase		2005 Hg emission (Mg yr^{-1})	
			Oxidation	Oxidation	Reduction	Anthropogenic	Natural & Secondary
CMAQ-Hg (v. 4.6)	N. Hemisphere	108 km × 108 km	O_3, OH, H_2O_2, Cl, Cl_2	O_3, OH, HOCl/OCl^-	SO_3^{2-}, hν, HO_2	1635	2537
GRAHM (v. 1.1)	Global	1 deg. × 1 deg.	O_3, Br, BrO, Cl, Cl_2	O_3, OH, HOCl/OCl^-	SO_3^{2-}, hν	1925	3500
GLEMOS (v. 1.0)	Global	5 deg. × 5 deg.	O_3, OH, Br, BrO, Cl_2	O_3, OH, HOCl/OCl^-	SO_3^{2-}	1925	4230

GMDD
4, 1723–1754, 2011

Table 2. Summary of observation networks used in this study.

Observation Network	Key Parameter	Unit	Data Completeness [a] (%)	Frequency	Site #	Type	Region	Source
CARIBIC	TGM [b]	ng m^{-3}	n/a	every 10–15 min	n/a	aircraft	Asia, Europe, South America	Brenninkmeijer (2009)
CAMNet	TGM [b]	ng m^{-3}	0.06–97.59	hourly	11	surface	North America	Environment Canada (2005)
EANET	Precip. [c]	mm	50.00–100.00	daily or weekly	43	surface	East Asia	ACAP (2010)
EMEP	Precip. [c]	mm	72.60–100.00	weekly-bimonthly	15	surface	Europe	Hjellbrekke (2010)
	$Hg^{d}_{(aq)}$	ng L^{-1}	72.60–100.00	weekly-bimonthly	13			
	TGM [b]	ng m^{-3}	14.25–98.90	hourly-monthly	8			
	Hg^{Te}	ng m^{-3}	23.84–78.36	hourly-biweekly	5			
	Hg^{0f}	ng m^{-3}	86.14	hourly	1			
	Hg^{IIg}	pg m^{-3}	6.08	hourly-daily	1			
	Hg^{Ph}	pg m^{-3}	6.08–100.00	hourly-biweekly	4			
MDN	Precip. [c]	mm	11.45–100.00	daily-monthly	95	surface	North America	NADP (2010)
	$Hg^{d}_{(aq)}$	ng L^{-1}	11.45–100.00	daily-monthly	95			

Note: [a] Data completeness is defined as percentage of available data in one year;
[b] TGM is total gaseous mercury ($Hg^0 + Hg^{II}$);
[c] Precip. is precipitation;
[d] $Hg_{(aq)}$ is total mercury in precipitation;
[e] Hg^T is total mercury in the air ($Hg^0 + Hg^{II} +, Hg^P$);
[f] Hg^0 is gaseous elemental mercury;
[g] Hg^{II} is gaseous divalent mercury;
[h] Hg^P is particulate-bound mercury.

GMDD
4, 1723–1754, 2011

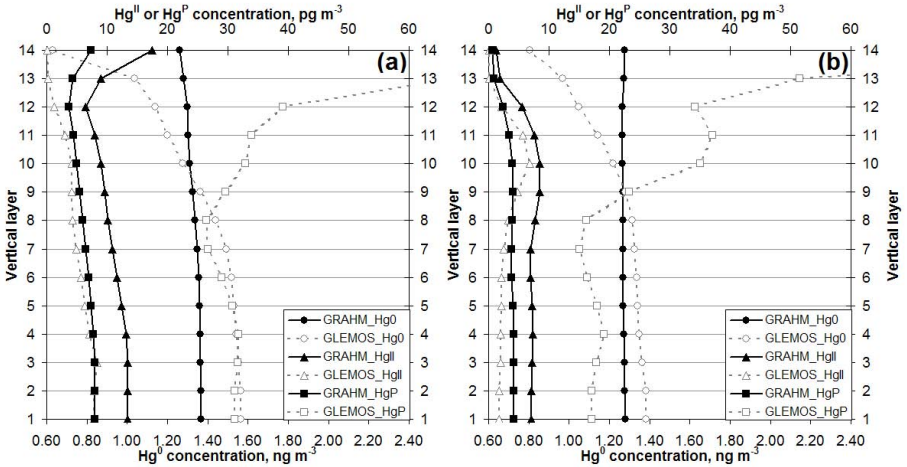

Fig. 1. Vertical profile of IC/BC for Hg species from the global models **(a)** mean of IC in the CMAQ hemispheric domain and **(b)** annual mean of BC from the domain boundary.

GMDD
4, 1723–1754, 2011

Application of CMAQ at a hemispheric scale

P. Pongprueksa et al.

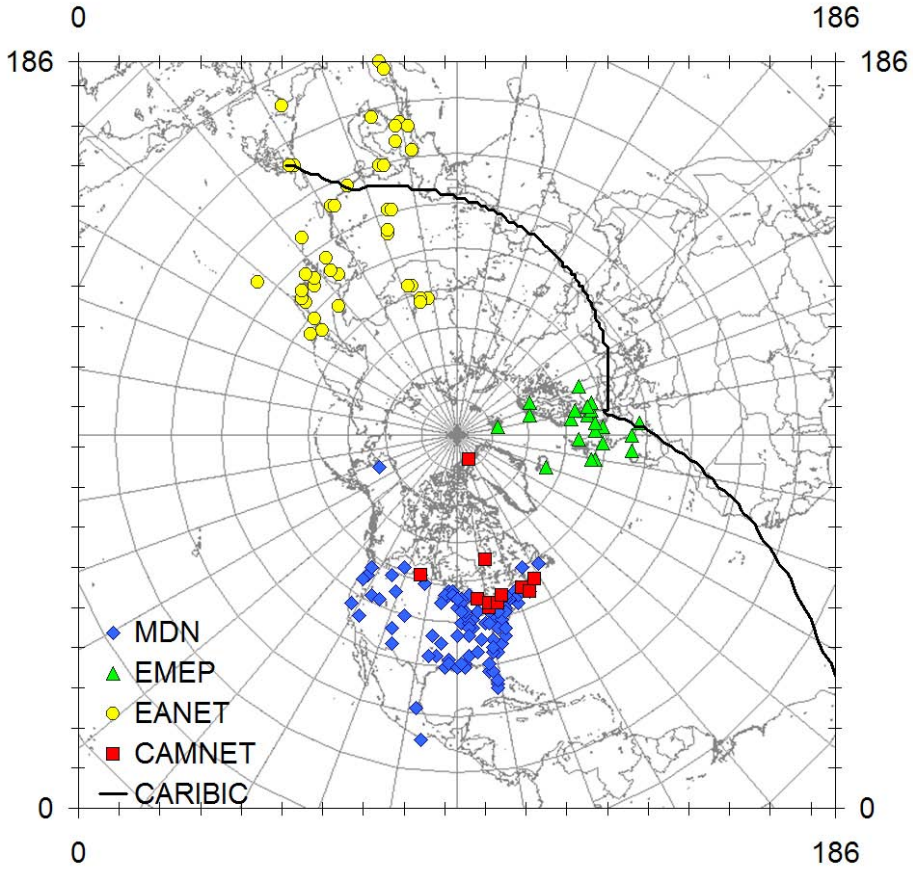

Fig. 2. CMAQ modeling domain, ground-based monitoring sites, and simplified CARIBIC flight trajectories.

GMDD
4, 1723–1754, 2011

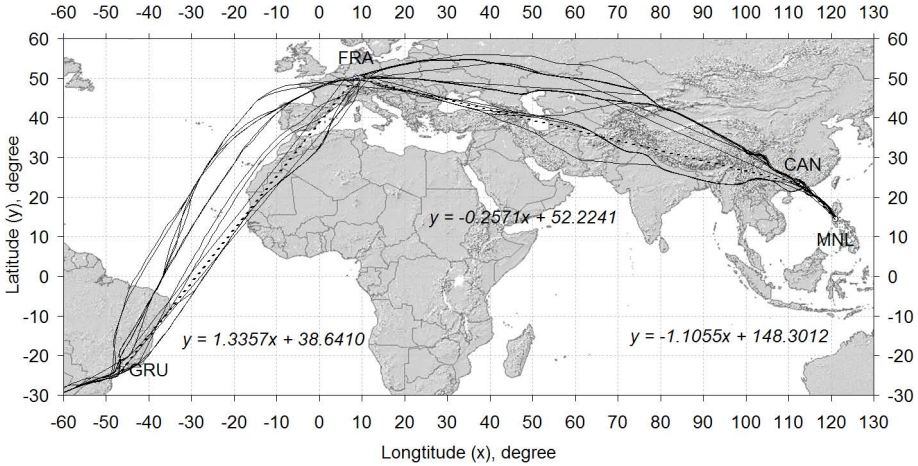

Fig. 3. Actual CARIBIC trajectories (solid lines) and simplified flight tracks (dotted lines).

GMDD
4, 1723–1754, 2011

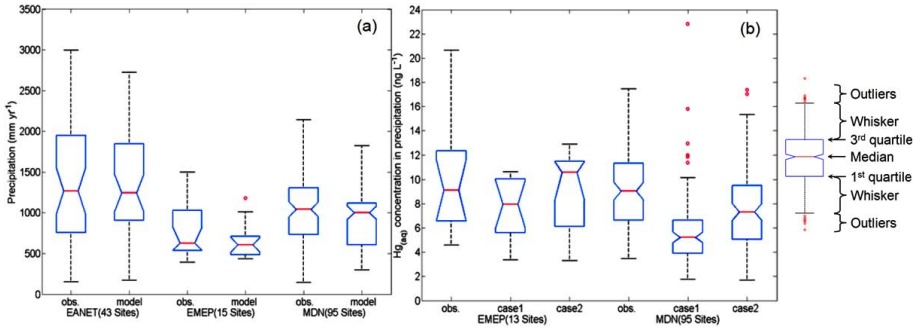

Fig. 4. Box plots of data from observation networks and model simulations **(a)** annual precipitation and **(b)** aqueous Hg concentration in precipitation.

GMDD
4, 1723–1754, 2011

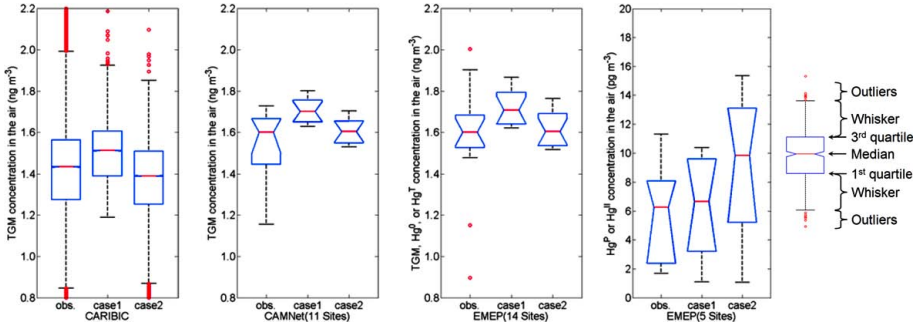

Fig. 5. Box plots of Hg species concentrations in the atmosphere from aircraft measurements, ground-based measurements, and model simulations.

GMDD
4, 1723–1754, 2011

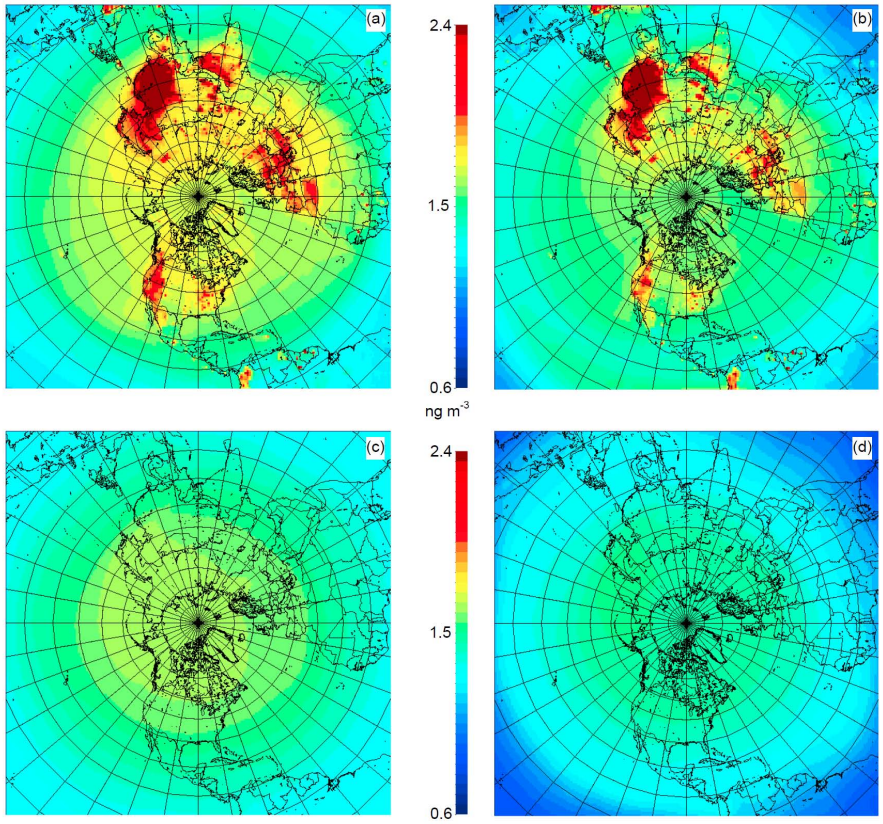

Fig. 6. Annual average TGM concentrations **(a)** GRAHM-CMAQ at ground level **(b)** GLEMOS-CMAQ at ground level **(c)** GRAHM-CMAQ at aircraft level **(d)** GLEMOS-CMAQ at aircraft level.

GMDD
4, 1723–1754, 2011

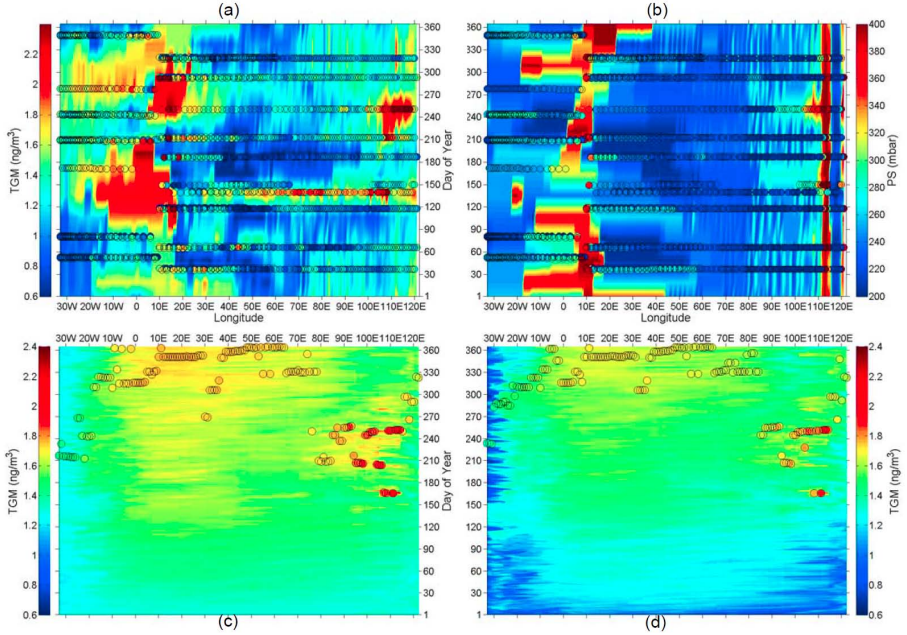

Fig. 7. Filled contour plots gridded in longitude and day of year showing **(a)** CARIBIC TGM concentration [measurement data points in bubbles], **(b)** CARIBIC static pressure [measurement data points in bubbles], **(c)** GRAHM-CMAQ TGM concentration [max. values in bubbles], and **(d)** GLEMOS-CMAQ TGM concentration [max. values in bubbles]. Note: for each Julian day (Y Axis), the values of the shown parameters represent the measured/model-predicted concentration/pressure along the flight trajectory of that day in terms of longitude. For example, in Fig. 7a and b, the CARIBIC measurements were performed monthly and shown in bubbles; the rest of the contour plot was interpolated using the measured data.

GMDD
4, 1723–1754, 2011

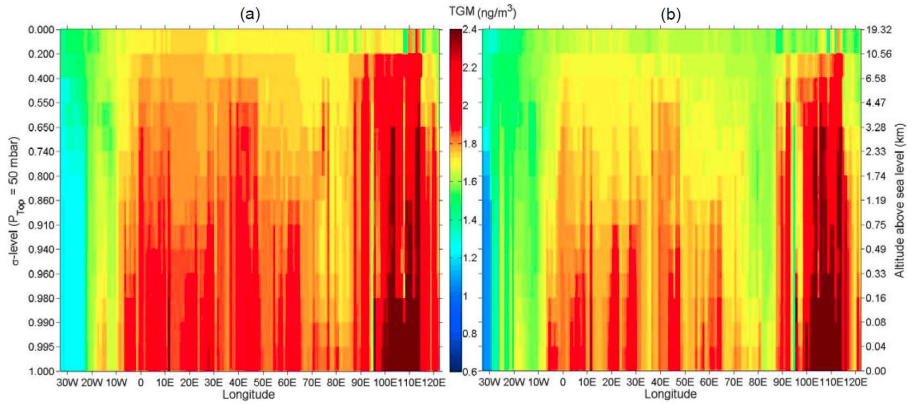

Fig. 8. Vertical profile for annual peaks of daily average TGM concentrations along the simplified flight-path derived from **(a)** GRAHM-CMAQ, and **(b)** GLEMOS-CMAQ. Note: for each vertical layer/altitude (Y Axis), the values represent simulated TGM concentration peaks of the year along the flight trajectory in terms of longitude.

GMDD
4, 1723–1754, 2011

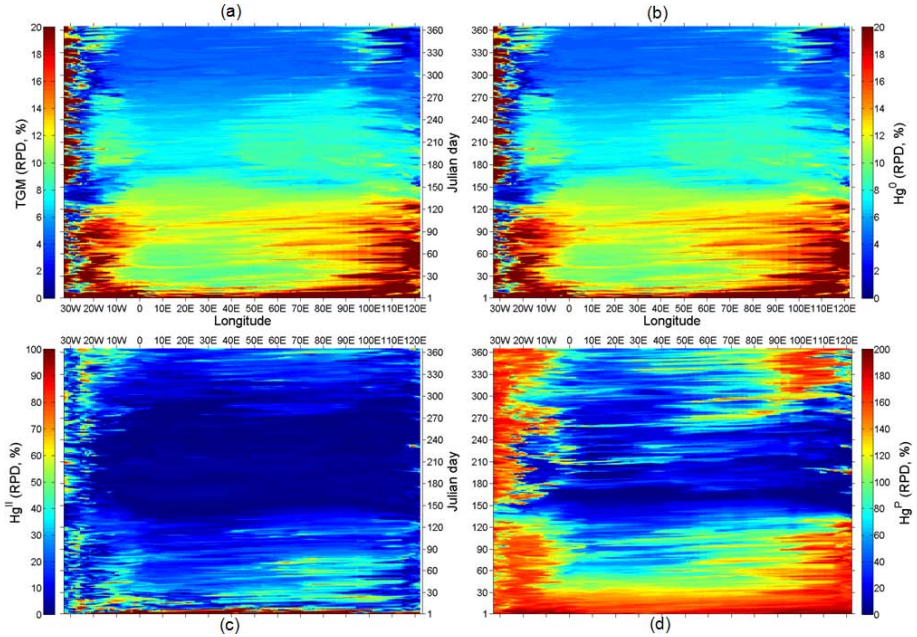

Fig. 9. The Relative Percent Difference of CMAQ data integrated with GRAHM and GLEMOS models **(a)** TGM, **(b)** Hg^0, **(c)** Hg^{II}, and **(d)** Hg^P. Note: for each Julian day (Y Axis), the values of the shown parameters represent the RPD between the two simulations of mercury species concentration along the flight trajectory of that day in terms of longitude.

GMDD
4, 1723–1754, 2011